Physical Layer Compact Models for Ring Resonators based Dense WDM Optical Interconnects

Sébastien Rumley, Meisam Bahadori, Dessislava Nikolova and Keren Bergman

Department of Electrical Engineering, Columbia University; New York, USA, rumley@ee.columbia.edu

Abstract T*wo compact models relating the coupling and attenuation coefficient of ring resonators to their physical dimensions are introduced. We leverage these models to delimit the capabilities of ring resonators for dense WDM optical interconnects.*

Introduction

The microring resonator (MRR) is often presented as the workhorse of future silicon photonics based optical interconnects. It has a limited footprint, and has been shown capable of a variety of functions: filtering, modulation, wavelength-selective dropping, and spatial switching[1,3]. Equipped with integrated heaters and feedback control loop, MRRs have been shown resistant to external thermal variations. Using a diode type junction for electrical drivers, nanosecond-scale tenability and switching have also been realized in MRRs.

These features have led to a variety of proposed compact WDM transmitters and receivers[2,3]. Numerous MRR-based networked architectures, acting as Networks-on-Chip (NoC)s, have also been promoted. In these designs, the MRR frequently appears as a discrete component achieving a specific function (e.g. selection of a single wavelength) at the cost of a predetermined power penalty. For an architecture to remain feasible, i.e. to ensure the power budget is respected[2], individual MRRs must generally inflict power penalties no larger than 1 dB.

The extensive usage of MRRs presented in certain studies, is however, questionable, as MRRs are subject to multiple constraints. MRRs must be large enough to prevent too high bending losses, especially when used in a drop configuration, but must remain small enough to avoid multiple resonances in the bandwidth of interest. Their coupling coefficients to the adjacent waveguides must be sufficient to capture the signal of interest, but not too high to avoid other signals being captured as well. Finally, the bandwidth of the ring should match the bandwidth of the transmitted signal. However, a too large bandwidth can cause a severe crosstalk problem if the channel density is high[3]. Under these multiple constraints, the selection of a ring with right parameters is not a straightforward process. Furthermore, in some cases no MRR matching all requirements exists. Methods permitting to identify whether rings matching the requirement can be fabricated, and how they should be designs, are therefore highly required. The design space of MRRs can be explored by means of abstract ring models[4,5]: a ring defined through a loss coefficient α, and one (filtering configuration) or two (add-drop configuration) coupling coefficient(s) κ_i describing the relationship with the surrounding waveguide(s). These models are key to seize the principles at play, yet they do not capture the relationships between fabrication and coefficients. As such, they are insufficient to clearly assess the capabilities of MRRs for optical interconnects in practice.

In this paper, we introduce two compact models to complement abstract ring models with a fabrication dimension. These simple models allow us to sweep a design space corresponding to different ring radii and gap sizes (i.e. distance separating the ring from the waveguide). For each considered ring, we calculate various figures of merit and exclude the designs failing to fulfil a set of minimal requirements. Finally, by considering the remaining "realm of feasibility", we derive conclusions on MRR capabilities.

Compact models

The first compact model relates the loss inflicted to signals transiting inside the MRR to its size. Theoretical models have been proposed to express the loss as a function of the ring radius but these models cannot include fabrication effects such as waveguide side-wall roughness[6]. Here we consider the bending loss as a fabrication-platform dependent relationship, to be obtained experimentally, and fitted. Such experimental measurements have been recently reported for the IME A*STAR 248nm process[7]. We fitted these measurements with a power law, aR^{-b}, where R is the ring radius (in micron units) and *a* and *b* are constant parameters. Hence, we assume the bending loss to be infinite for null radius and null for infinite radius (i.e. rectilinear waveguide). As shown in Fig. 1a, the fit (with parameters $a = 8.65 \cdot 10^7$ and $b = 8.135$) agrees reasonably well with the measurements. As indicated in [7], a radius independent propagation loss must be added to the bending

loss. The loss model thus becomes α (dB/cm) = $aR^{-b} + c$. Our *baseline* compact model for loss considers the aforementioned *a* and *b* values, and *c* = 2 dB/cm. We also define a *pessimistic* loss model with the same *a* and *b* values and *c* = 8 dB/cm (corresponding to a waveguide with doped heaters[7]). Finally, we also fitted simulation results presented in [7] for a quasi-ideal design with a 90nm slab, and obtained $a' = 1.09 \cdot 10^9$ and $b' = 10.15$. Combined with an optimized waveguide loss of *c* = 1dB/cm [8], these values constitute the *optimistic* ring loss model.

The second proposed compact model intends to capture the relationship between the gap size separating an MRR from the waveguide and the coupling coefficient κ. We approximate the ring-waveguide coupling region as a rectilinear

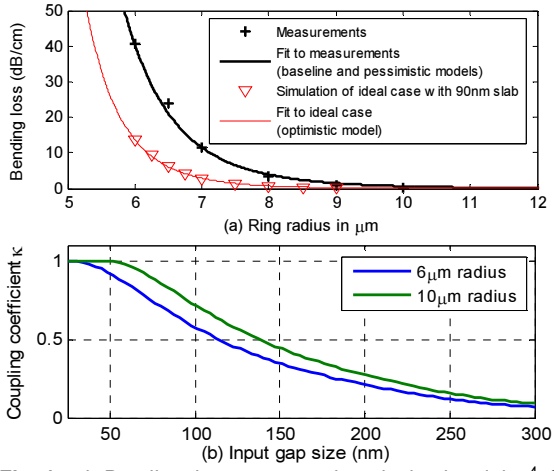

Fig 1: a) Bending loss measured and simulated in [4] for various radii, and associated power law fits used in the three defined ring loss models. **b)** Impact of input gap size on coupling coefficient.

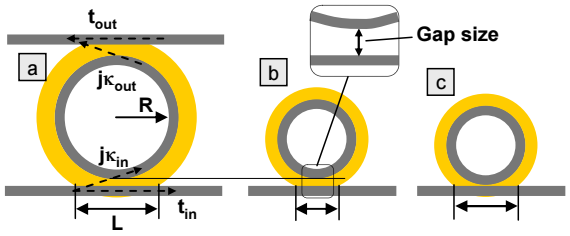

Fig 2: Impact of radius and gap size on coupling length L. a) and b) have same gap sizes but the smaller diameter of b) results in a shorter approximated coupling length. b) and c) are of equal diameter but different gap sizes, resulting in different coupling lengths, and distinct coupling coefficients κ and t.

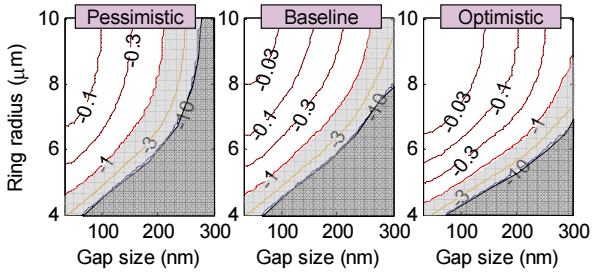

Fig 3: Insertion loss (dB) at resonant frequency (IL_{drop}), for various ring designs, and considering three loss models.

coupler. To estimate its length, we calculate the penetration depth of the optical mode around the ring as a function of the mode refractive indexes at a reference wavelength (1550nm throughout this paper). We then calculate the length of the waveguide that falls within this penetration depth (Fig. 2). This is done by means of trigonometric analysis, and by assuming that the ring is perfectly circular, thus leading to minimized round trip losses. On the other hand, we used COMSOL to simulate directional couplers for several gap sizes, obtained the effective indexes seen by odd and even supermodes ($n_{eff,even}$, $n_{eff,odd}$), and found two polynomial interpolations. When applied to a particular ring geometry, the model first calculates the length of the coupling region L, obtains the $n_{eff,odd}$ and $n_{eff,even}$, and finally evaluates the coupling coefficient:

$$\kappa = \sin\left(2\pi \frac{L}{\lambda} \frac{n_{eff,even} - n_{eff,odd}}{2}\right). \qquad (1)$$

Coupling coefficients obtained with this model are shown in Fig 1b. Note that our polynomial interpolations agree well with COMSOL simulations for gap sizes up to 300nm, but diverge for larger values. However, as shown in Fig. 1b, for a gap size of 300nm the coupling is very weak and, as exemplified hereafter, such designs have limited interest.

Design exploration

Although our models are applicable to various design scenarios, we focus in this paper on wavelength add-drop rings, as the ones used to demultiplex WDM signals at the receiver side[3]. Being passive (thermal stabilization taken apart), they operate as linear time-invariant filters, which makes modelling more straightforward. Add-drop rings are defined by three geometrical parameters: input and output gap sizes, and radius. In order for signals tuned to the resonant wavelengths to be effectively dropped, the critical coupling condition must be fulfilled, i.e. $l = t_{in}^2/t_{out}^2 = (1-\kappa_{in}^2)/(1-\kappa_{out}^2)$, where l is the round trip loss in the ring. As κ_{in}, κ_{out} depend on the gap sizes, and l on the radius, this condition dictates the size of the output gap when the radius and the input gap are set.

We applied our models to various radii (from 4 to 10μm) and for various input gap sizes (from 30 to 300nm). With the loss and coupling coefficients returned by our compact models, we first evaluate the attenuation (in dB units) at resonant frequency, generally referred to as IL_{drop} (Fig. 3). The dark gray regions comprise cases where critical coupling cannot be attained. The light gray regions indicate designs where critical coupling can be attained but at the price

of a significant insertion loss (>1dB). The impact of the loss model is clearly apparent. In the *pessimistic* case, no design in the explored space shows an IL_{drop} inferior to 0.03dB. In the *optimistic* case, the smallest radius limiting the loss below 1dB is 4.4μm, instead of 4.7 μm for both *baseline* and *pessimistic* cases.

We then evaluated the attenuation (in dB units) experienced by non-resonant frequencies in the pass by path (IL_{thru}). As thru attenuation depends almost exclusively on the coupling coefficient, only the results corresponding to the *baseline* loss model are displayed. Fig. 4a shows the attenuation at FSR/2, i.e. at the frequency located exactly in between two resonances (ideal case). Since thru insertion losses are typically accumulated across a demultiplexing array or rings, the effect of each ring should be kept low, (e.g. below 0.1 dB - light gray region in Fig. 4a). Fig 4b, in contrast, shows the attenuation for a detuning of 1nm, corresponding to the nearest channel in a medium density WDM scenario. The effect of ring corresponding to the nearest channel should also be kept below 1dB (light gray in Fig. 4b). This requirement is more constraining than the one imposed in Fig. 4a in the space explored. It further raises the minimum radius leading to acceptable performances to 4.85μm, (*optimistic*) and 5.35μm (*baseline* and *pessimistic*).

Figure 5, finally, depicts the region of the design space that remains when designs falling in any gray zone are removed. Also indicated is the 3-dB bandwidth of each remaining design. We observe that with the pessimistic loss model, the design space is narrow. Also, the minimal bandwidth is 23GHz (corresponding to a gap size of 208nm, Q-factor ~8580). This is narrow enough to properly isolate 10G channels in a demultiplexer array[3], but also requires the radius of the ring to be larger than 9μm, thus limiting the FSR to 9nm. For the baseline case, smallest radii are of 6.5μm, but lead to bandwidths >50GHz (due to the small input gap of 157nm). To reduce this bandwidth, e.g. to 20 GHz, while ensuring that IL_{drop} < 1dB, the radius and the input gap must be raised to 7.6μm and 215nm respectively. By increasing the input gap only, the bandwidth is reduced, as well as the IL_{thru}, but the IL_{drop} increases to -3.4dB.

This analysis illustrates how our proposed compact models can be leveraged to explore the design space of microring resonators. We aim at refining them, and at validating them against more measurements in the near future.

Conclusions

We presented two compact models to relate the physical dimensions and fabrication imperfections of MRRs to theoretical parameters κ (coupling coefficient) and α (loss coefficient). In particular, we proposed a power law model for the bending loss. We applied these compact models to a wide set of designs. Results show that with ring losses corresponding to current fabrication capabilities, ring radii cannot be smaller than ~7μm, thereby limiting the FSR to ~12.74nm. Compact models as the ones presented here can be integrated in a higher scale PDK and serve to evaluate and optimize large architectures composed of many rings.

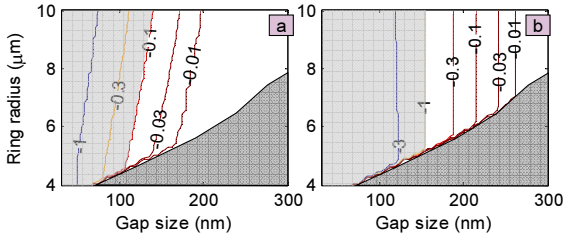

Fig 4: a) Insertion loss for non-dropped signals (IL_{thru}), at FSR/2, in dB **b**) Insertion loss for frequency showing a 1nm detuning with resonant frequency, in dB.

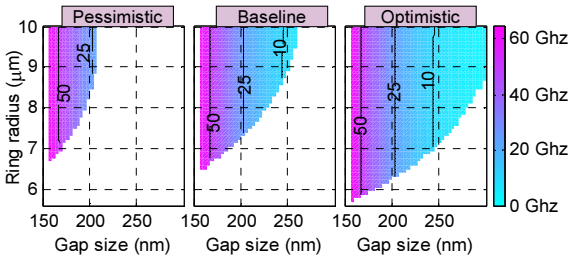

Fig 5: Regions of interest with different ring loss models. Designs leading to unacceptable insertion losses have been removed. Color reflects 3-dB bandwidth of the ring.

Acknowledgements

This work is supported in part by the U.S. Department of Energy (DoE) National Nuclear Security Administration (NNSA) through contract PO1426332 with Sandia National Laboratories. This work is also supported by an Early Stage Innovations grant from NASA's Space Technology Research Grants Program.

References

[1] B. A Small, et al. "Multiple-wavelength integrated photonic networks based on microring resonator devices", J. of Optical Netowrking. Vol 6, no. 2 (2007).

[2] R. Hendry, et al. "Physical Layer analysis and modeling of silicon photonic WDM bus architectures", HiPEAC workshop, Vienna, Austria, (2014).

[3] M. Bahadori et al. "Comprehensive Design Space Exploration of Silicon Photonic Interconnects" IEEE. J. Lightwave Tech., in press (2016).

[4] D. G. Rabus, "Integrated Ring Resonators: The Compendium", Springer (2007).

[5] W. Bogarts, et al. "Silicon microring resonators", Laser Photonics Rev. 6, No 1 (2012).

[6] Y. A. Vlasov et al., "Losses in single-mode silicon-on-insulator strip waveguide and bends" Opt. Exp., Vol. **12**, no. 8, (2004).

[7] H. Jayatilleka et al., "Crosstalk in SOI Microring Resonator-Based Filters" IEEE. J. Lightwave Tech., in press (2016).

[8] K. Yamada "Silicon Photonic Wire Waveguides: Fundamentals and Applications" Silicon Photonics II, Components and Integration, Springer (2011).